

## Supporting Information

**Predictably Engineering the Viscoelastic Behavior of Dynamic Hydrogels via Correlation with Molecular Parameters**

*Junzhe Lou, Sean Friedowitz, Karis Will, Jian Qin, Yan Xia*

Dr. J. Lou, K. Will, Prof. Y. Xia

Department of Chemistry, Stanford University, Stanford, California 94305, United States

Dr. J. Lou, Dr. S. Friedowitz,

Department of Materials Science and Engineering, Stanford University, Stanford, California 94305, United States

Prof. J. Qin

Department of Chemical Engineering, Stanford University, Stanford, California 94305, United States

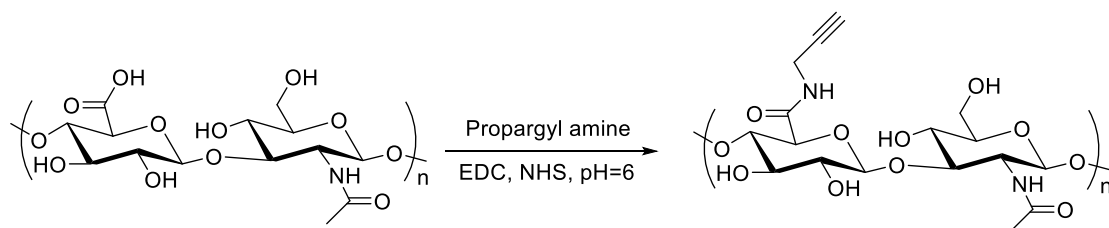
## General Information

**Materials.** Sodium hyaluronates (39 kDa, 45 kDa, 74 kDa) were purchased from Lifecore Biomedical. 4-arm 10 kDa PEG-OH (hydroxyl terminal groups), 8-arm 20 kDa PEG-OH, 4-arm 10 kDa PEG-amine hydrochloride and 8-arm 20 kDa PEG-amine hydrochloride were purchased from Jenkem Technology USA. All other chemicals were obtained from commercial sources and used as received unless otherwise noted. 2-(2-(2-(azidoethoxy)ethoxy)ethoxy)acetaldehyde (**S1**) was prepared according to literature procedures.<sup>[1]</sup> N-(3-azidopropyl)-2-hydrazineylacetamide (**S2**) was synthesized as previously reported. Analytical thin-layer chromatography (TLC) was carried out using 0.2 mm silica gel plates (silica gel 60, F254, EMD chemical).

**Characterizations.** <sup>1</sup>H and <sup>13</sup>C NMR spectra were recorded using 400 Varian NMR spectrometers. Chemical shifts are reported in ppm using the residual protiated solvent as an internal standard (CDCl<sub>3</sub> <sup>1</sup>H: 7.26 ppm and <sup>13</sup>C: 77.0 ppm; D<sub>2</sub>O <sup>1</sup>H: 4.79 ppm; DMSO-d<sub>6</sub> <sup>1</sup>H: 2.50 ppm and <sup>13</sup>C: 39.5 ppm). Rheological characterization was performed using an AR-G2 controlled stress rheometer at 37 °C. All measurements were performed using an 8 mm parallel plate geometry and analyzed using TRIOS Software. Tensile and compression tests were performed using Instron (model 3342 with a load cell of maximum 50N). HPLC-MS was performed in acetonitrile/water containing 0.1% formic acid on an Alliance e2695 Separations Module using an XBridge 10 μm C18 column in series with a 2489 UV/Visible Detector.

## Experimental Section

1. Hyaluronic Acid (HA) modification*HA modification with alkyne*

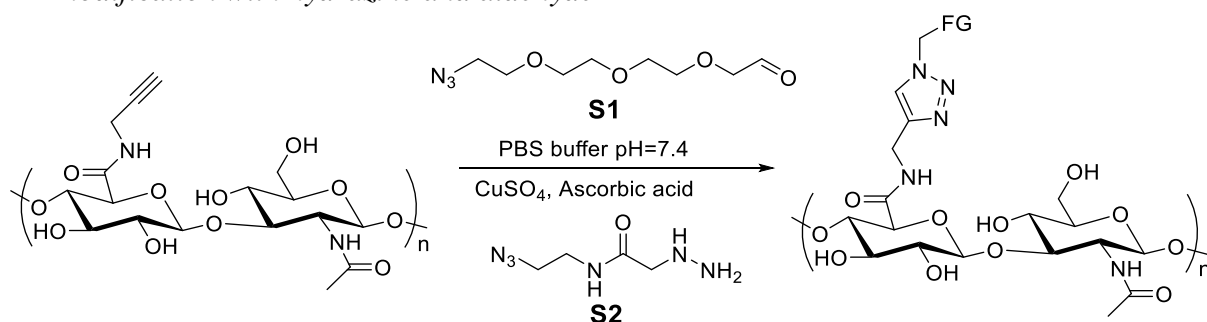


**HA-alkyne of 12% modification:** Sodium hyaluronate (1 g) was dissolved in MES buffer (0.2 M, pH 4.5) to a concentration of 10 mg/mL. To this solution, N-hydroxysuccinimide (NHS, 223 mg per gram of HA, 0.8 eq. to the HA dimer unit), 1-ethyl-3-(3-dimethylaminopropyl) carbodiimide (EDC, 372 mg per gram HA, 0.8 eq.) and propargyl amine (128  $\mu$ L per gram HA, 0.8 eq.) were added successively. After adjusting pH to 6, the mixture was stirred at room temperature for 4 h. The solution was then dialyzed against DI water for 3 d and lyophilized to give a white powder.

**HA-alkyne of 15% modification:** Sodium hyaluronate (1 g) was dissolved in MES buffer (0.2 M, pH 4.5) to a concentration of 10 mg/mL. To this solution, NHS (334.5 mg per gram of HA, 1.2 eq. to the HA dimer unit), EDC (558 mg per gram HA, 1.2 eq.) and propargyl amine (192  $\mu$ L per gram HA, 1.2 eq.) were added successively. After adjusting pH to 6, the mixture was stirred at room temperature for 4 h. The solution was then dialyzed against DI water for 3 d and lyophilized to give a white powder.

**HA-alkyne of 20% modification:** Sodium hyaluronate (1 g) was dissolved in MES buffer (0.2 M, pH 4.5) to a concentration of 10 mg/mL. To this solution, NHS (418 mg per gram of HA, 1.5 eq. to the HA dimer unit), EDC carbodiimide (697.5 mg per gram HA, 1.5 eq.) and propargyl amine (240  $\mu$ L per gram HA, 1.5 eq.) were added successively. After adjusting pH to 6, the mixture was stirred at room temperature for 4 h. The solution was then dialyzed against DI water for 3 d and lyophilized to give a white powder.

#### HA modification with hydrazine and aldehyde



HA-alkyne (300 mg) was dissolved in phosphate buffered saline (pH 7.4) at 2 wt% followed by the addition of azido-aldehyde (**S1**) or azido-hydrazine (**S2**) (100 mg, 1 eq. to HA dimer unit). The solution was then bubbled with  $N_2$  for 30 min. Copper (II) sulfate pentahydrate (0.76 mg, 0.004 eq. to HA dimer unit) and sodium ascorbate (8.7 mg, 0.06 eq. to HA dimer unit) were dissolved in DI water, bubbled with  $N_2$ , and added to HA solution. After stirring at room temperature for 1 d, the mixture was dialyzed against DI water for 3 d and lyophilized. The degree of modification on HA was quantified using  $^1H$  NMR spectroscopy by integration of the proton signal on triazole group ( $\delta = 7.85$ , 1H) relative to that of the methyl groups on N-acetylglucosamine of HA backbone ( $\delta = 1.8$ , 3H).  $^1H$  NMR integration indicated that 12 - 20% of the carboxylate groups on the HA backbone have been functionalized (Figure S3-5).

## 2. Modification of Polyethylene Glycol (PEG)

**4-arm or 8-arm PEG-aldehyde:** 4-arm and 8-arm PEG-aldehyde was synthesized by Dess-Martin oxidation. Dess Martin periodinane (255 mg, 1.5 eq. to hydroxyl groups) was added to the dichloromethane (DCM, 8 mL) solution of 4-arm or 8-arm PEG-OH (1 g). The mixture was stirred at room temperature overnight. After filtering through celite, the solution was concentrated and precipitated in diethyl ether. The crude product was then dissolved in water, dialyzed against DI water for 3 d and lyophilized to give a white powder.

**4-arm or 8-arm PEG-hydrazine:** 4-arm and 8-arm PEG-hydrazine was synthesized by reacting PEG-NH<sub>2</sub> and tri-Boc-hydrazinoacetic acid NHS ester followed by Boc-deprotection. Tri-Boc-hydrazinoacetic acid NHS ester was first synthesized via carbodiimide coupling. Tri-Boc-hydrazinoacetic acid (2.5 g, 6.4 mmol, 1 eq.), *N*-hydroxysuccinimide (0.81 g, 7.1 mmol, 1.1 eq.), 1-ethyl-3-(3-dimethylaminopropyl)carbodiimide (1.6 g, 8.3 mmol, 1.3 eq.), and 4-dimethylaminopyridine (0.16 g, 1.3 mmol, 0.2 eq.) were dissolved in 10 mL DCM. The solution was stirred at room temperature overnight. The solvent was removed under reduced pressure, and the residue was purified by silica gel chromatography (ethyl acetate/hexane, 1:1 v/v) to obtain the product as white solid (2.9 g, 94% yield). 4-arm or 8-arm PEG-amine hydrochloride (700 mg), trimethylamine (58  $\mu$ L, 1.5 eq. to amine) and tri-Boc-hydrazinoacetic acid NHS ester (273 mg, 2 eq. to amine) were dissolved in DCM (7 mL). After stirring at room temperature overnight, the solution was concentrated, precipitated in diethyl ether twice and dried under vacuum. The solid was then dissolved in a mixture of DCM/trifluoroacetic acid (1:1, 10 mL) for Boc-deprotection. The solution was stirred at room temperature for 4 h, concentrated and then precipitated in diethyl ether. The crude product was dissolved in water, dialyzed against DI water for 3 d and lyophilized to give a white powder.

## 3. Hydrogel Preparation

Stock solutions of hydrazine and aldehyde modified HA or PEG were first solubilized in PBS (10X, pH 7.4) at 5 wt% respectively. Catalyst **1** was dissolved in PBS (10X, pH 7.4) and adjusted pH to 7.4 at a stock concentration of 500 mM. HA hydrogels were prepared by mixing HA-hydrazine, catalyst, and HA-aldehyde stock solutions successively at hydrazine to aldehyde ratio of 1:1. PEG hydrogels were prepared by mixing PEG-hydrazine, catalyst, and PEG-aldehyde stock solutions successively at hydrazine to aldehyde ratio of 1:1. The volumes of stock solutions were adjusted to make gels with different formulations.

## 4. Rheological Tests

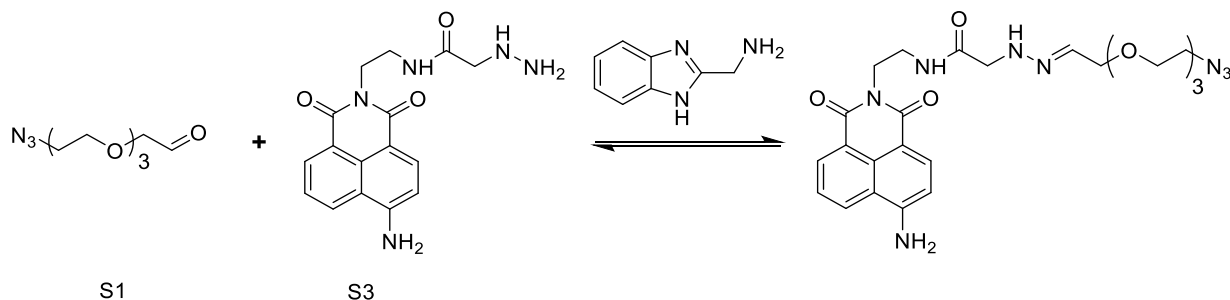
Rheological characterization was performed on a stress-controlled rheometer (AR-G2, TA instrument) using an 8 mm parallel plate. 50  $\mu$ L of a sample was loaded immediately onto the rheometer before gelation and the exposed gel surfaces were coated with mineral oil to prevent dehydration. All the tests were performed at 37°C. Time sweeps were performed at 1 Hz at 1% constant strain. Frequency sweeps were performed from 0.01 to 10 rad/s at 1% constant strain. Stress relaxation experiments were performed at 10% strain.

## 5. Tensile and Compression Tests

For tensile and hysteresis tests, rectangular hydrogels (10  $\times$  10  $\times$  1 mm<sup>3</sup>) were prepared and stretched on an Instron mechanical tester. The strain rate was 30 mm/min for tensile tests and 1 mm/min for hysteresis

tests. For compression tests, disks of hydrogels were punched out (8 mm diameter, 1 mm thickness) and measured using an Instron mechanical tester at a strain rate of 10 mm/min.

### 6. Kinetic Measurement of Hydrazone Exchange by HPLC



Kinetics of a model reaction between aldehyde S1 and hydrazine S3 were studied using HPLC. S3 was synthesized by coupling N-(2-aminoethyl)-4-amino-1,8-naphthalimide<sup>[2]</sup> with hydrazine using carbodiimide chemistry. 2 mM stock solutions of hydrazine and aldehyde were prepared in a PBS buffer (1X, pH 7.4). A 250 mM stock solution of catalyst was prepared in PBS.

The appropriate amounts of catalyst, hydrazine, and aldehyde were sequentially added to PBS buffer (1X, pH 7.4) from their stock solutions, maintaining the same concentrations for hydrazine and aldehyde. The reactions were performed at 37°C in a water bath and monitored using HPLC with detection at 420 nm absorption (HPLC conditions: XBridge 10  $\mu$ m C18 column; 40% acetonitrile in PBS buffer (pH 7) isocratic elution in 7 min at a flow rate of 0.34 mL/min. The reactant concentrations and conversions were calculated from the integrals of the HPLC signals. The kinetic data of hydrazone formation were fitted to the standard kinetic model for 2<sup>nd</sup> order reactions using Matlab (Figure S1).<sup>[3]</sup>

### 7. Model Fitting of Stress Relaxation

Conversion between the stress-relaxation modulus and the complex modulus was performed according to the schematic in Figures 2c and 2d. We first fit the experimentally obtained  $G(t)$  data with a multi-exponential generalized Maxwell model,

$$G(t) = \sum_i g_i \exp(-t/\tau_i)$$

where  $\tau_i$  are individual relaxation times and  $g_i$  are the contribution of each mode obtained from fitting. The above multi-exponential sum smoothens the experimental data and facilitates the numerical conversion of the stress relaxation curve to the frequency domain. It is inspired by but should not be regarded as a direct application of a physical model. A set of evenly log-spaced  $\tau_i$  are chosen across the range of experimental  $G(t)$  time signals. This range of relaxation times is limited by the time-discretization and overall length of  $G(t)$  signal, which subsequently limits the upper and lower frequency peaks present in the complex modulus spectra. We generally observe a set of peaks in the spectra in the range of  $\tau_i \approx 10^3$  to  $10^5$  s, depending on the molecular weight, degree of modification, and catalyst concentration. The obtained spectra for each sample and the calculated relaxation times are found to be insensitive to the exact mode-spacing used in the fitting. We then use analytical formulas for the Fourier

transform of the  $G(t)$  model above to calculate the storage modulus ( $G'$ ) and loss modulus ( $G''$ ). These are represented in frequency space as,

$$G'(\omega) = \sum_i g_i \frac{\omega^2 \tau_i^2}{1 + \omega^2 \tau_i^2}$$

$$G''(\omega) = \sum_i g_i \frac{\omega \tau_i}{1 + \omega^2 \tau_i^2}$$

and are parameterized by the set of  $\tau_i$  and  $g_i$  obtained directly from fitting experimental data.

The range of highly contributed modes is generally quite narrow, resulting in attempts at fitting the  $G(t)$  data with molecular models such as the Sticky-Rouse models<sup>[4]</sup> compared to a multi-exponential fit.

Accurate conversion to the frequency domain requires a careful choice of the set of relaxation times  $\tau_i$  to capture the relaxation process. In previous works, distributions of relaxation times was used, with peaks in the distribution corresponding to physical processes in the system.<sup>[5]</sup> We, however, chose a set of  $\tau_i$  with a small logarithmic separation of  $\Delta = \log(\tau_i/\tau_{i-1}) = 0.1$ , and allowed the fit process for  $g_i$  to determine the contribution of each mode.

Additionally, the range of relaxation times fit to each sample is constrained to fall within the range of the initial and final experimental data points, to avoid introducing artifacts in the fit  $G(t)$  model due to extrapolation.

## References

- [1] M. Rubinshtein, C. R. James, J. L. Young, Y. J. Ma, Y. Kobayashi, N. C. Gianneschi, J. Yang, *Org. Lett.* **2010**, *12*, 3560-3563.
- [2] P. Remon, M. Hammarson, S. M. Li, A. Kahnt, U. Pischel, J. Andreasson, *Chem. - Eur. J.* **2011**, *17*, 6492-6500.
- [3] a) A. Dirksen, S. Dirksen, T. M. Hackeng, P. E. Dawson, *J. Am. Chem. Soc.* **2006**, *128*, 15602-15603; b) J. Lou, F. Liu, C. D. Lindsay, O. Chaudhuri, S. C. Heilshorn, Y. Xia, *Adv. Mater.* **2018**, *30*, 1705215.
- [4] Q. Chen, G. J. Tudryn, R. H. Colby, *J. Rheol.* **2013**, *57*, 1441-1462.
- [5] S. C. Grindy, R. Learsch, D. Mozhdehi, J. Cheng, D. G. Barrett, Z. B. Guan, P. B. Messersmith, N. Holten-Andersen, *Nat. Mater.* **2015**, *14*, 1210-1216.

## Supplemental Figures and Tables

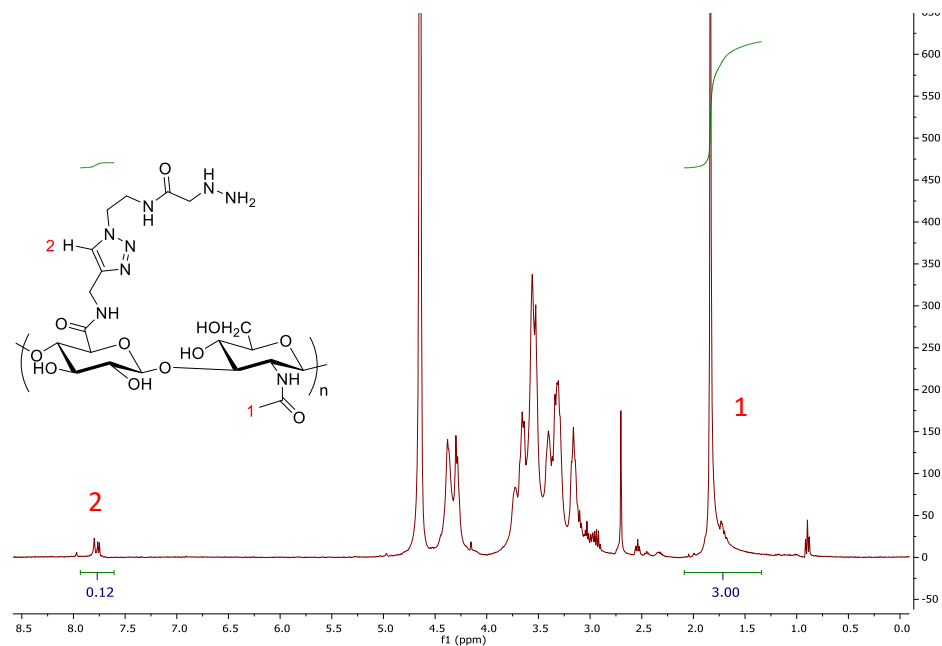


**Figure S1** <sup>1</sup>H NMR spectrum (D<sub>2</sub>O) of HA modified with hydrazine (HA-HYN) at 12% modification.

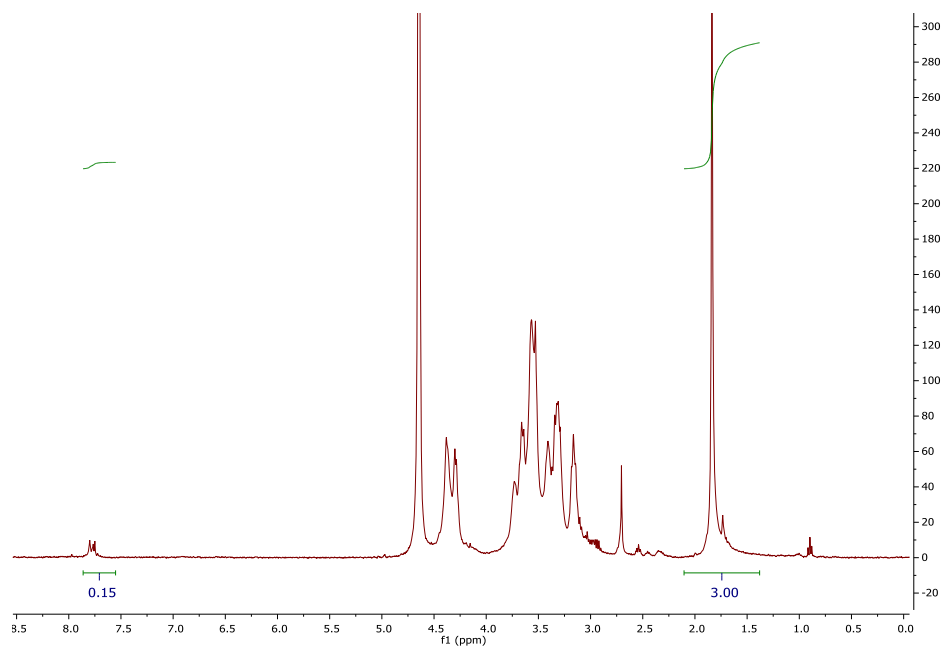


**Figure S2** <sup>1</sup>H NMR spectrum (D<sub>2</sub>O) of HA modified with hydrazine (HA-HYN) at 15% modification.

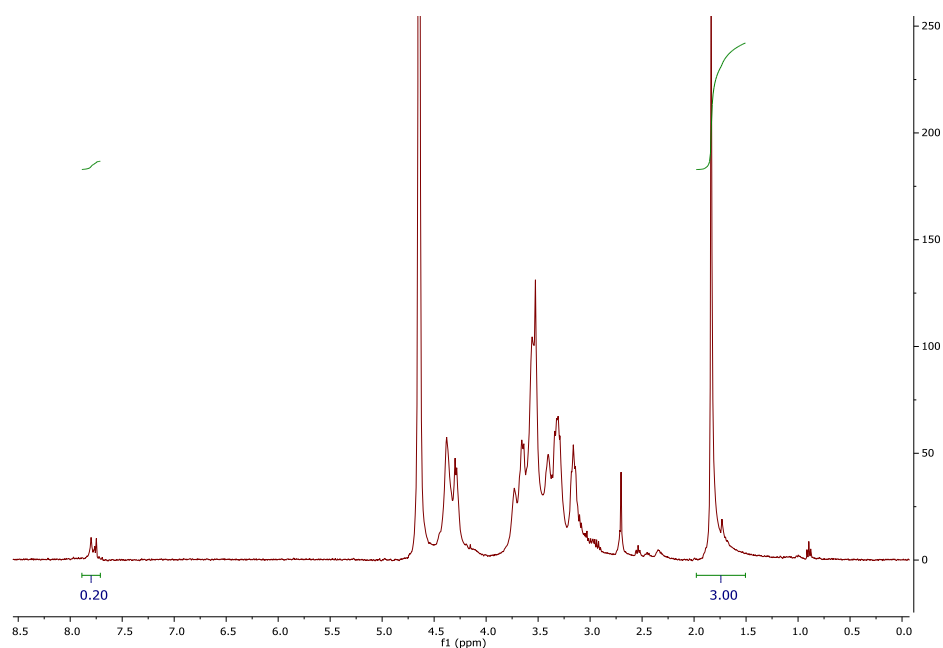


**Figure S3**  $^1\text{H}$  NMR spectrum ( $\text{D}_2\text{O}$ ) of HA modified with hydrazine (HA-HYN) at 20% modification.

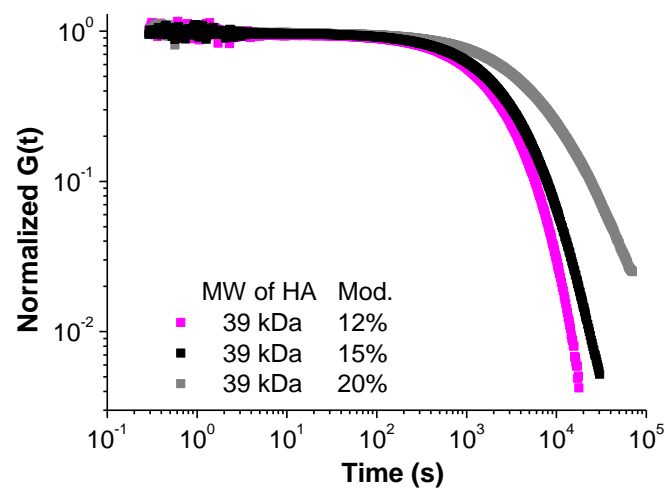


**Figure S4** Normalized stress relaxation curves of HA gels composed of HAs with different degrees of modification (12%, 15%, 20%).

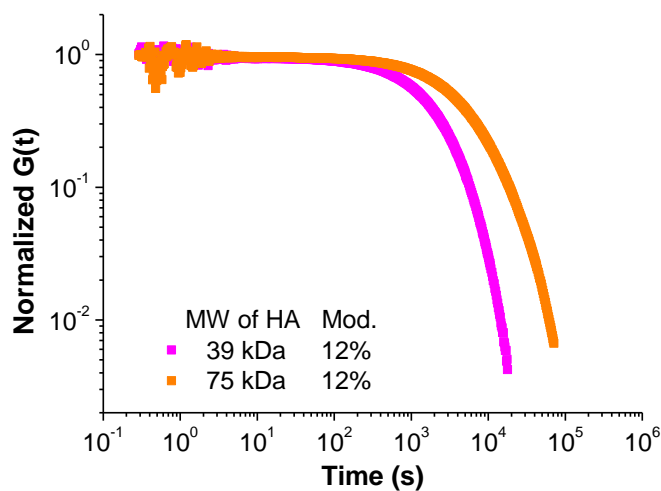


**Figure S5** Normalized stress relaxation curves of HA gels composed of HAs with different molecular weights (39 kDa, 75 kDa).

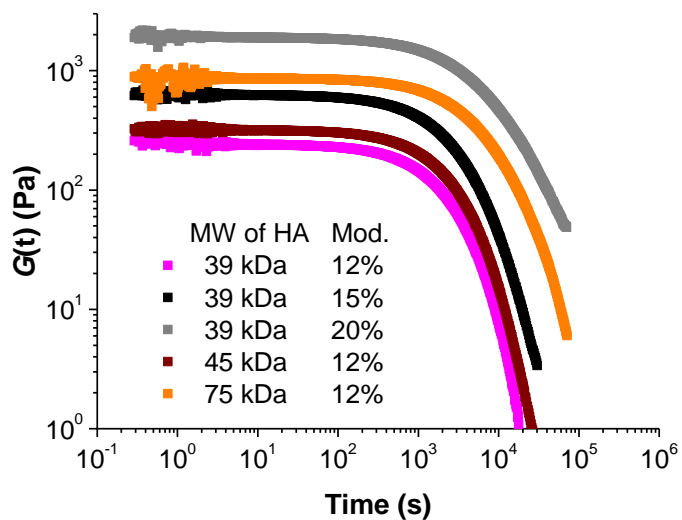


**Figure S6** Compiled stress relaxation curves of HA gels composed of HAs with different molecular weights and degrees of modification. The initial modulus increases with increasing molecular weight or degree of modification.



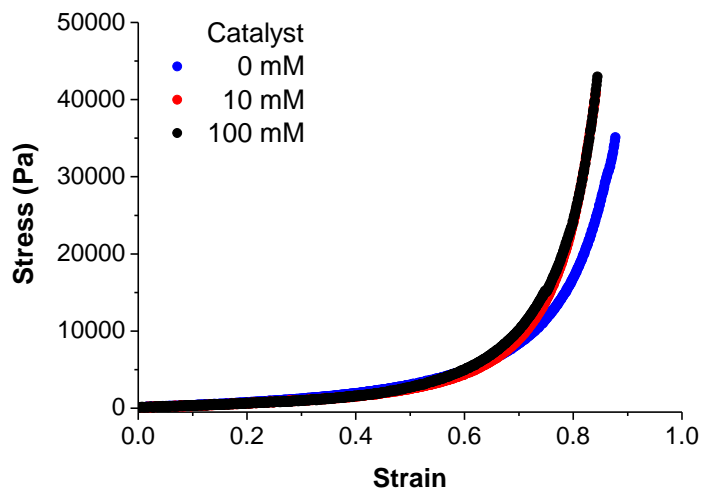


**Figure S7** Stress-strain curve of HA hydrogel (75 kDa, 12% functionalization, 2 wt%) with 0, 10 and 100 mM added under uniaxial compression, strain rate = 30 mm/min. The compression modulus is 3062 Pa (0 mM), 2794 Pa (10 mM), and 2717 Pa (100 mM).

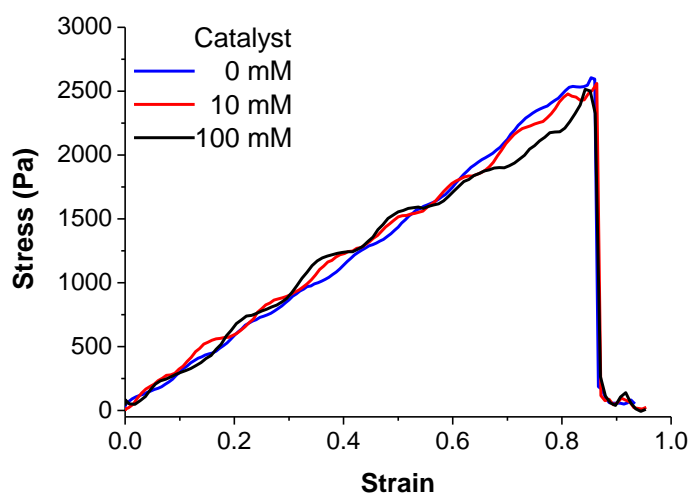


**Figure S8** Stress-strain curve of HA hydrogel (75 kDa, 12% functionalization) with 0, 10 and 100 mM added catalyst under uniaxial tension, strain rate = 30 mm/min. The elastic modulus is 3012 Pa (0 mM), 2917 Pa (mM) and 2743 Pa (100 mM).

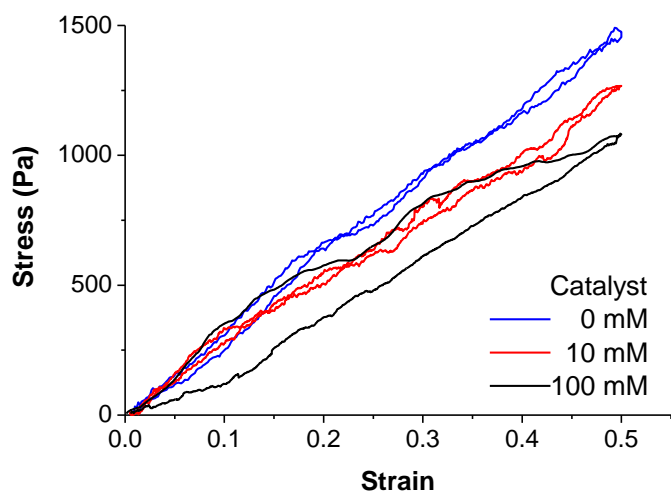


**Figure S9** Sequential loading-unloading cycle of HA hydrogel (75 kDa, 12% functionalization) with 0, 10 and 100 mM added catalyst under uniaxial tension at strain rate = 1 mm/min. A hysteresis loop was observed when 100 mM catalyst was incorporated in the hydrogel.

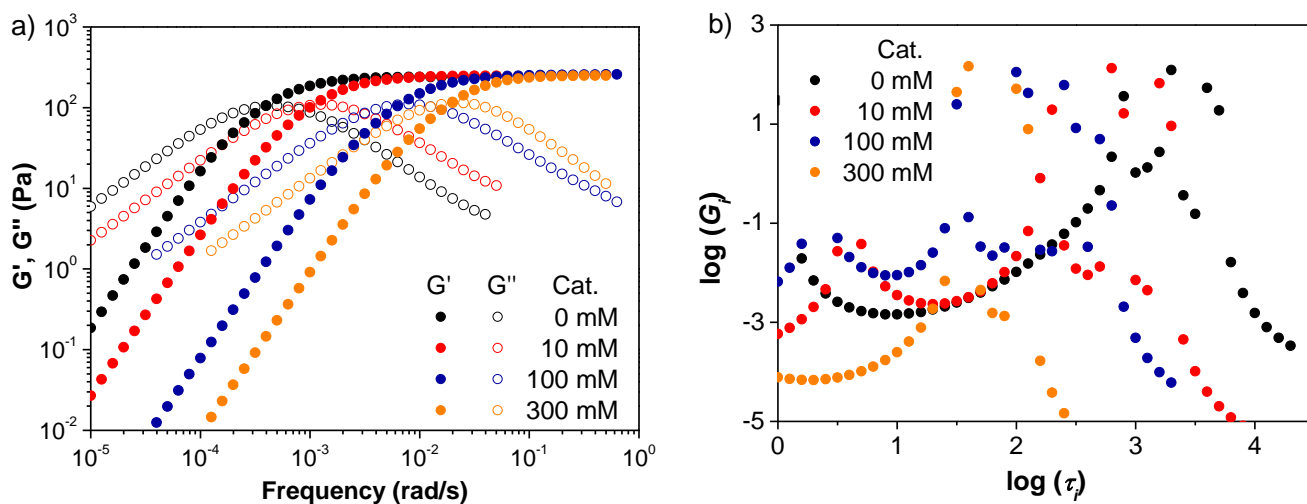


**Figure S10** Fitting results of stress relaxation curves from generalized Maxwell model for HAs of MW of 39 kDa and 12% modification at different catalyst loadings. a) Oscillatory frequency sweep data converted from stress relaxation profiles by fitting and interpolation method. b) Model fitting with logarithmic separations with different relaxation time  $\tau_i$  in Maxwell models.

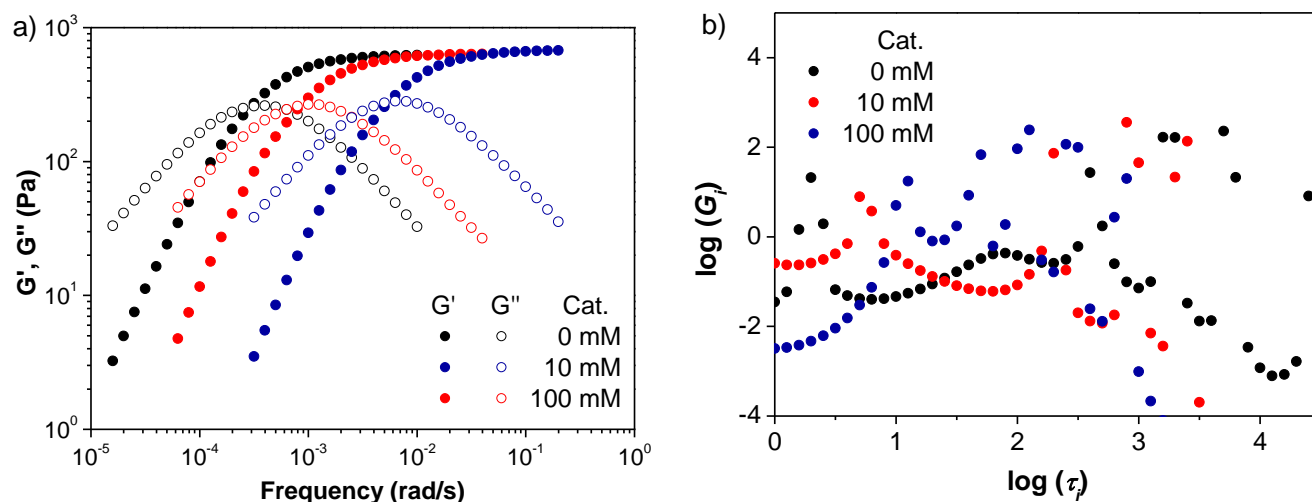


**Figure S11** Fitting results of stress relaxation curves from generalized Maxwell model for HAs of MW of 39 kDa and 15% modification at different catalyst loadings. a) Oscillatory frequency sweep data converted from stress relaxation profiles by fitting and interpolation method. b) Model fitting with logarithmic separations with different relaxation time  $\tau_i$  in Maxwell models.

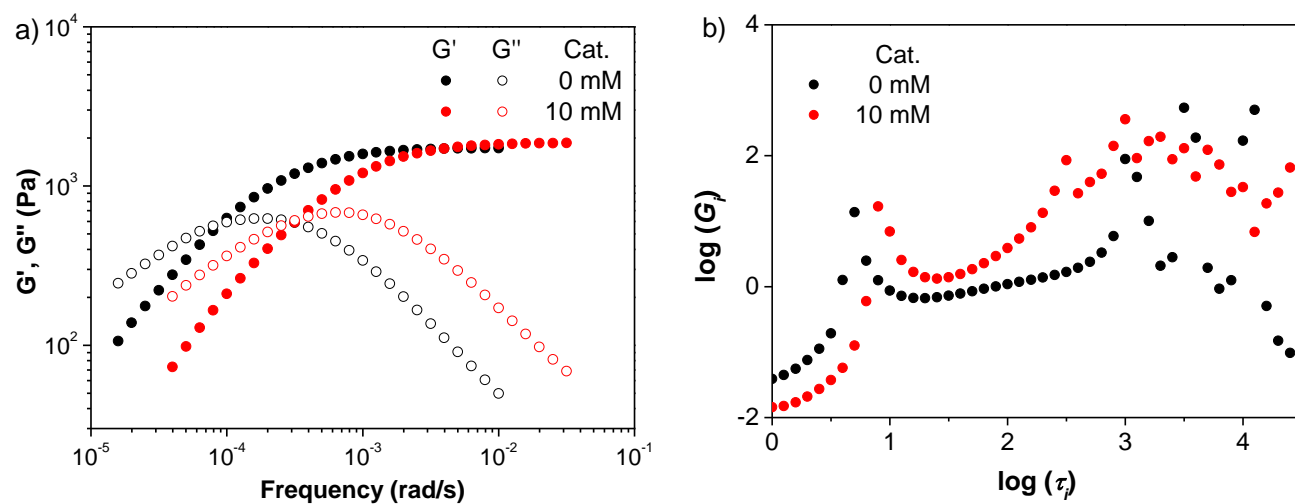


**Figure S12** Fitting results of stress relaxation curves from generalized Maxwell model for HAs of MW of 39 kDa and 20% modification at different catalyst loadings. a) Oscillatory frequency sweep data converted from stress relaxation profiles by fitting and interpolation method. b) Model fitting with logarithmic separations with different relaxation time  $\tau_i$  in Maxwell models.

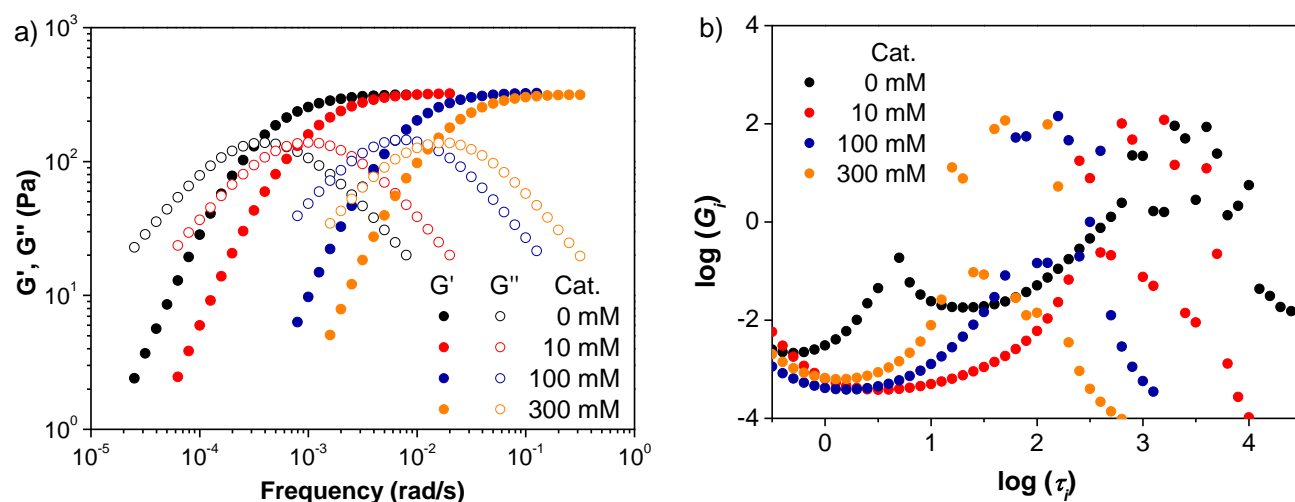


**Figure S13** Fitting results of stress relaxation curves from generalized Maxwell model for HAs of MW of 45 kDa and 15% modification at different catalyst loadings. a) Oscillatory frequency sweep data converted from stress relaxation profiles by fitting and interpolation method. b) Model fitting with logarithmic separations with different relaxation time  $\tau_i$  in Maxwell models.

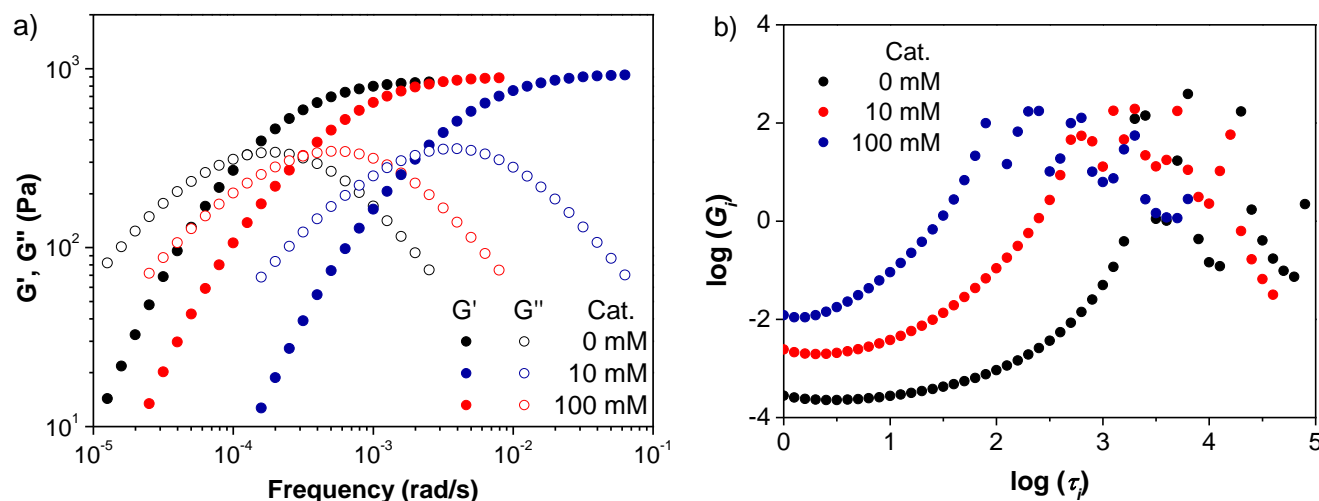


**Figure S14** Fitting results of stress relaxation curves from generalized Maxwell model for HAs of MW of 75 kDa and 15% modification at different catalyst loadings. a) Oscillatory frequency sweep data converted from stress relaxation profiles by fitting and interpolation method. b) Model fitting with logarithmic separations with different relaxation time  $\tau_i$  in Maxwell models.

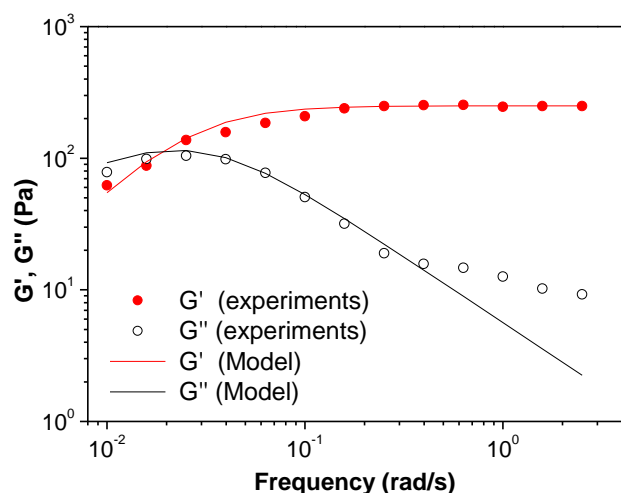


**Figure S15** Oscillatory frequency sweep of HA hydrogel (35 kDa, 12% functionalization).

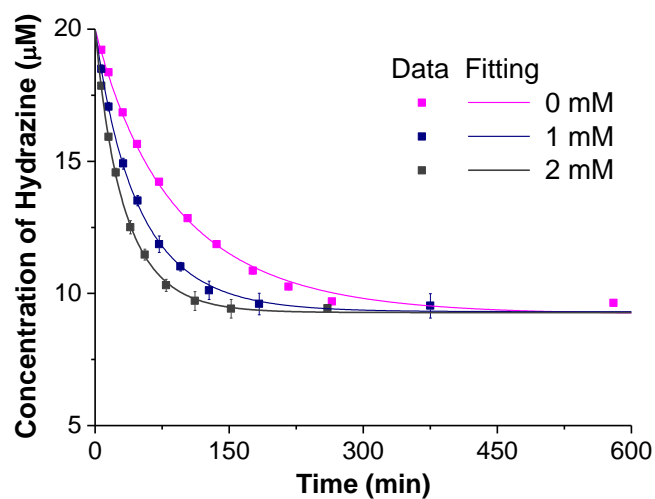


**Figure S16** Conversion of hydrazine and aldehyde to hydrazone in model reactions at 20  $\mu\text{M}$  reactants at 37  $^{\circ}\text{C}$  in PBS buffer (1X, pH 7.4) in the presence of 0 (pink), 1 (navy), and 2 mM (gray) catalyst **1**. Each data point represents the mean value from three independent kinetics tests. The solid line represents the fitting of raw data using the 2<sup>nd</sup> order reversible reaction kinetics model.

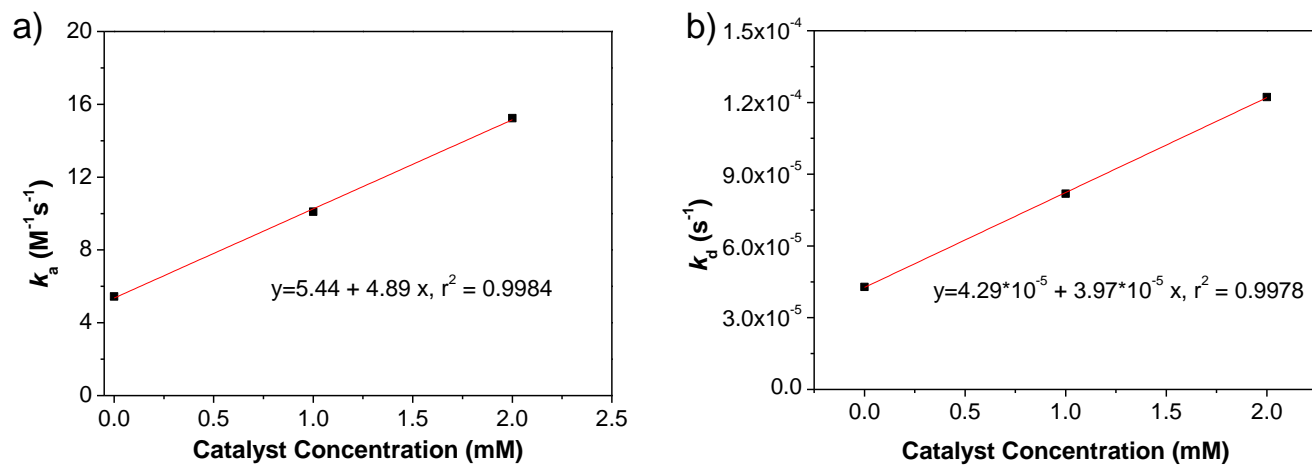


**Figure S17** Linear dependence of a) association rate ( $k_a$ ) and b) dissociation rate ( $k_d$ ) on catalyst concentration.

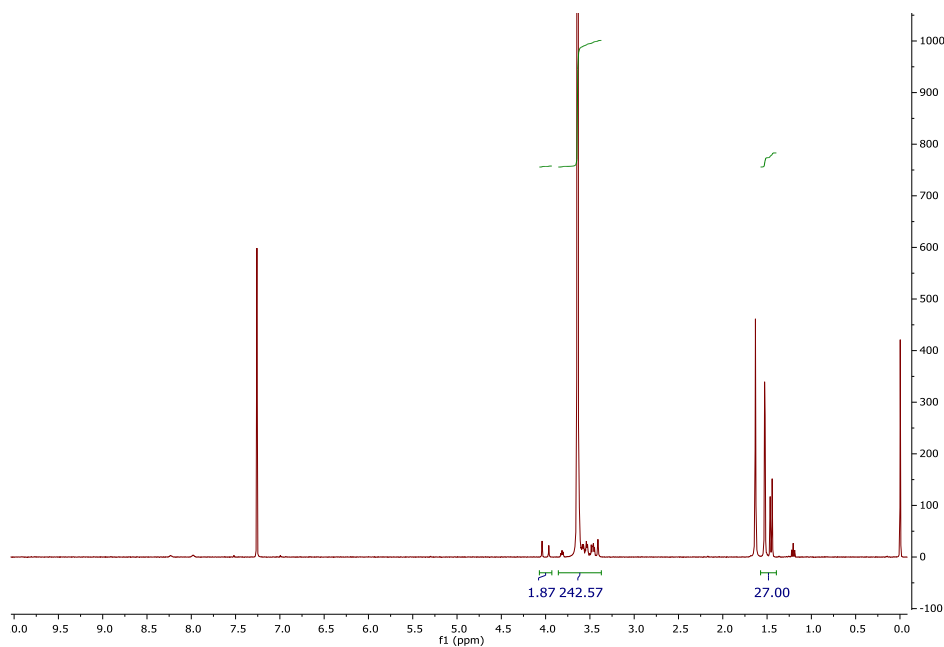


**Figure S18** <sup>1</sup>H NMR spectrum (CDCl<sub>3</sub>) of 4-arm PEG-Boc-hydrazine.

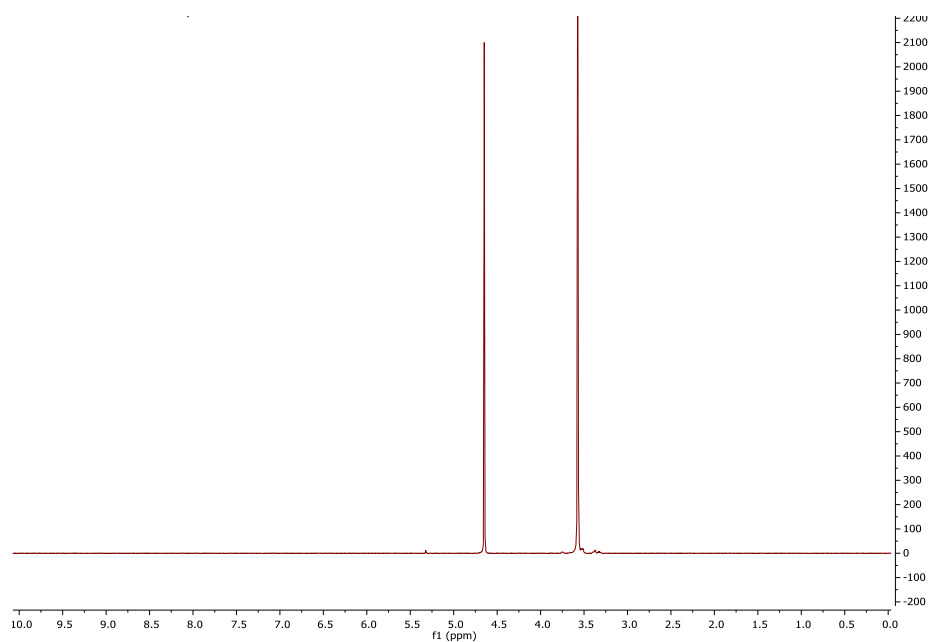


**Figure S19**  $^1\text{H}$  NMR spectrum ( $\text{D}_2\text{O}$ ) of 4-arm PEG-hydrazine.

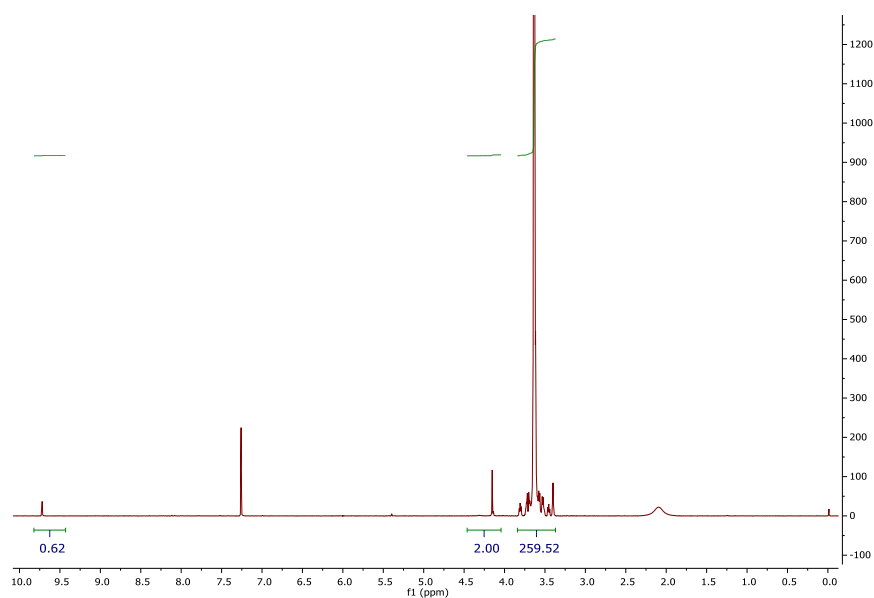


**Figure S20**  $^1\text{H}$  NMR spectrum ( $\text{CDCl}_3$ ) of 4-arm PEG-aldehyde.

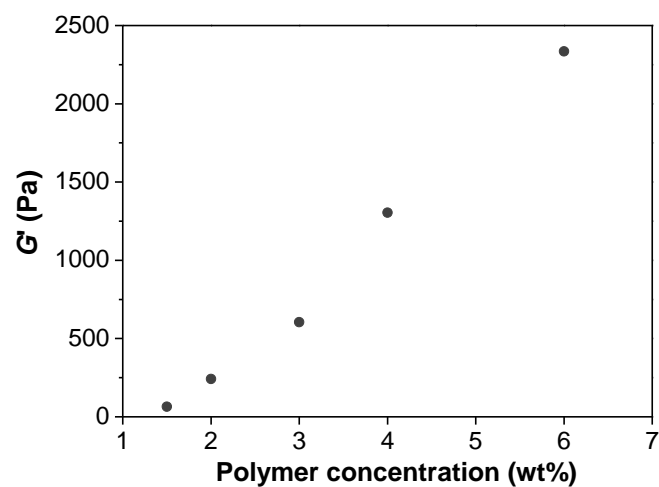


**Figure S21**  $G'$  of hydrogels using 39 kDa HA with 12% functionalization at HA concentrations of 1.5, 2, 3, 4 and 6 wt%.

**Table S1** Storage modulus ( $G'$ ) of HA hydrogels at different polymer concentrations at 1 Hz.

HA concentration	$G'$ (Pa)
1.5 %	65
2 %	242
3 %	604
4 %	1304
6 %	2334



**Table S2.**  $k_a$ ,  $k_d$  and  $K_{eq}$  at different catalyst concentrations. Rate constants were directly measured at 0 and 2 mM catalyst loading and calculated based on linear dependence at 5, 10, 100, 300 mM catalyst loading.

[Cat] (mM) <sup>a</sup>	$k_a$ (M <sup>-1</sup> s <sup>-1</sup> )	$k_d$ (s <sup>-1</sup> )	$K_{eq}$ (M <sup>-1</sup> ) <sup>b</sup>	1/ $k_d$ (s)
0	5.44	4.29×10 <sup>-5</sup>	1.27×10 <sup>5</sup>	23310
2	15.2	1.22×10 <sup>-4</sup>	1.24×10 <sup>5</sup>	8197
5	29.8	2.41×10 <sup>-4</sup>	1.24×10 <sup>5</sup>	4147
10	54.3	4.39×10 <sup>-4</sup>	1.24×10 <sup>5</sup>	2278
100	495	4.01×10 <sup>-3</sup>	1.24×10 <sup>5</sup>	249
300	1472	1.19×10 <sup>-2</sup>	1.24×10 <sup>5</sup>	84

<sup>a</sup> concentration of the catalyst, aminomethyl benzimidazole. <sup>b</sup>  $K_{eq}$  was calculated by  $k_a/k_d$ .

**Table S3** Average effective crosslinks ( $N_s$ ) for HAs with different molecular weights and degrees of modification.

$N_s$	Molecular Weight (kDa)	Degree of Modification
11	39	12%
14	39	15%
19	39	20%
13	45	12%
21	75	12%

**Table S4** Storage modulus ( $G'$ ) of 4-arm PEG hydrogels at different polymer concentrations at 1 Hz.

PEG concentration	$G'$ (Pa)
1.5 %	75
2 %	220
4 %	1953
8 %	9108

**Table S5** Corresponding molar ratio of catalyst to hydrazine and weight percentage (wt%) of catalyst in HA hydrogels for different catalyst concentrations.

Degree of functionalization	[Cat] (mM)	[Cat]/[Hydrazine]	Weight percentage wt%
<b>12%</b>	2	0.68	0.037
<b>12%</b>	5	1.7	0.092
<b>12%</b>	10	3.4	0.18
12%	100	34.2	1.8
12%	300	102.5	5.5
15%	10	3.4	0.18
15%	100	34.2	1.8
20%	10	3.4	0.18

**Table S6** Corresponding molar ratio of catalyst to hydrazine and weight percentage (wt%) of catalyst in PEG hydrogels for different catalyst concentrations.

[Cat] (mM)	[Cat]/[Hydrazine]	Weight percentage wt%
<b>2</b>	0.5	0.037
<b>5</b>	1.25	0.092
<b>10</b>	2.5	0.18
<b>100</b>	25	1.8
<b>300</b>	75	5.5